This is an *Accepted Manuscript*, which has been through the Royal Society of Chemistry peer review process and has been accepted for publication.

Accepted Manuscripts are published online shortly after acceptance, before technical editing, formatting and proof reading. Using this free service, authors can make their results available to the community, in citable form, before we publish the edited article. We will replace this *Accepted Manuscript* with the edited and formatted *Advance Article* as soon as it is available.

You can find more information about *Accepted Manuscripts* in the **Information for Authors**.

Nanoscale

ARTICLE

Tunable doping of graphene nanoribbon arrays by chemical functionalization

Pablo Solís-Fernández,[a] Mark A. Bissett,[a,‡] Masaharu Tsuji[a] and Hiroki Ago[a,b,*]

We demonstrate the controlled tuning of the electronic band structure of large-arrays of graphene nanoribbons (GNRs) by chemical functionalization. The GNR arrays are synthesized by substrate-controlled metal-assisted etching of graphene in H_2 at high temperature, and functionalized with different molecules. From Raman spectroscopy and carrier transport measurements, we found that 4-nitrobenzenediazonium (4-NBD) and diethylene triamine (DETA) molecules can tune the doping level of the GNR arrays to p- and n-type, respectively. In both cases, the doping effects induced in the GNRs were found to be higher than for a pristine graphene sheet, due to the presence of a large quantity of edges. Effects of chemical doping on the Raman spectrum of sp^2 carbon materials are also discussed. Our findings offer an effective way to control the electronic structure of GNRs by chemical functionalization, and are expected to facilitate the production of nanoribbon-based p-n junctions for future implementation into electronic circuits.

Introduction

Although graphene is expected to become one of the most significant materials in the field of technology in the upcoming years, more work still needs to be done to adjust its properties to the requirements of the electronic industry. Particularly, a lot of effort has been made trying to overcome the problems originating from the lack of a bandgap in the electronic structure of graphene. Several ways to open such bandgap have been proposed, including the application of electrical fields to double-layer graphene,[1] mechanically straining single-layer graphene,[2] different kinds of chemical functionalization,[3–5] and the one-dimensional quantum confinement of the charge carriers in the graphene nanoribbons (GNRs).[6–18] Among these, the synthesis of GNRs is one of the most promising approaches, due to the possibility to control the magnitude of the bandgap by a precise tuning of the width and edges of the GNRs.

Several methods have been employed to synthesize GNRs, either by bottom-up or top-down approaches. Bottom-up methods include the dehydrogenation reaction of surface-polymerized molecules,[8] and the direct growth by chemical vapor deposition (CVD) processes on transition metals.[11,12,14] On the other hand, top-down methods generally rely on the patterning of a graphene sheet/flake using different lithography and plasma etching processes.[10,13,16,17] Unzipping of carbon nanotubes by plasma or acid treatment is also an effective way to obtain GNRs.[6] While top-down approaches present the advantage of providing nanoribbons in a large-scale, the edges of the GNRs are generally damaged because plasma treatments are frequently used to etch the graphene sheet or the carbon nanotubes. Some of the mentioned approaches allow for the production of aligned arrays of GNRs, thus facilitating the production of multichannel field-effect transistor (FET) devices.[10–13,15–17] Multichannel devices are able to sustain higher currents than devices with an isolated ribbon in the conducting channel, and their higher surface area makes them suitable candidates for improved large-area molecular sensors.[17]

In addition to the control of the bandgap, tuning of other electrical properties of the graphene, such as the carrier type and concentration, and the Fermi level, is also important for electronic applications.[19] In that regard, controlled modulation of the doping level to either p- or n-type is desirable for a wide range of technological applications, including electronic/optoelectronic applications,[20] molecular sensing,[21] and the design of logic circuits.[22] Chemical functionalization has proved to be an effective method to modulate the density of holes and electrons for several graphitic materials, including graphene and GNRs.[3,5,9,19,21,23–35] Diazonium molecules are frequently used to functionalize graphene and carbon nanotubes.[5,9,23–26,28–31,36–39] Functionalization with diazonium salts usually proceeds by the grafting of the aryl groups to the graphene network, and thus changes the sp^2 hybridization of the involved carbon atoms to sp^3.[32] One of the advantages of functionalization with diazonium molecules is that opposite doping effects are expected to occur depending on the nature of the functional groups attached to the benzene ring.[25,28,31,38] In this sense, hole doping of graphene has been extensively reported by functionalization with 4-nitrobenzenediazonium (4-NBD), which contains an electron withdrawing nitro group.[24,25,28,29,31] On the other hand, electron doping of graphene can be realized by using a wide variety of molecules containing different nitrogen groups.[3,19,27] Recently, different ethylene amines have been shown to produce n-doping in graphene by a simple procedure.[35]

In the present work, for the first time, we demonstrate the possibility to tune the doping level of dense arrays of aligned GNRs by chemical functionalization. The GNRs have been prepared by substrate-controlled metal-assisted etching of graphene, thus avoiding the use of harsh plasma treatments. Functionalization of the GNRs involved two molecules, namely 4-NBD and diethylene triamine (DETA), and the effects of functionalization were monitored by Raman and x-ray photoelectron (XPS) spectroscopies, and by measuring the carrier transport properties of the GNRs. Our results show that 4-NBD and DETA allow the controlled tuning of the carrier type in GNR multichannel FETs. The doping effect in the GNRs is found to be higher than that in pristine graphene, due to the presence of a high density of edges to which a preferential attachment or binding of these molecules occurs.[19,36] While functionalizations of covalent nature are generally more stable, non-covalent approaches are better for preserving the properties of graphene as no structural damage is produced in its structure.[3,21,27,32,35] In the case of our GNRs, we will see that, thanks to the role of the edges in the functionalization, covalent approaches can be realized without further degrading the electronic properties of the GNRs. Our results are expected to be developed to future electronic/optoelectronic applications of GNRs.

Experimental section

The aligned GNRs were produced by metal-assisted etching of graphene, following our previously reported procedure.[15] In brief, large-area, single-layer graphene was grown by CVD on a Cu film sputtered on sapphire c-plane.[40] The CVD grown graphene was then spin-coated with PMMA and transferred to a sapphire r-plane substrate, which is responsible of producing aligned etching during the subsequent annealing. Removal of PMMA was done by washing in acetone overnight. After the sputtering of Ni nanoparticles at room temperature, the graphene supported on the sapphire r-plane was annealed in an Ar/H$_2$ flow at 400 °C and 1100 °C for 1 hour and 30 minutes, respectively. During the annealing at 1100 °C, the substrate-controlled etching of the graphene is catalyzed by the deposited Ni nanoparticles, producing densely-packed arrays of aligned nanoribbons with average widths of ~19 nm and in densities that go up to ~25 μm^{-1}.[15] Structural characterization of the GNRs was done by atomic force microscopy (AFM) in a Multimode scanning probe microscope (SPM) with a Nanoscope V controller (Bruker Co.), and by scanning electron microscopy (SEM, S-4800, Hitachi High-Technologies Co.).

Prior to the functionalization experiments, the as-produced GNR arrays were immersed in an aqueous solution of HCl to remove residual Ni particles. Successful removal of Ni was later confirmed by the absence of a related signal in the XPS spectra, collected in a Kratos Axis 165 spectrometer equipped with a monochromatic Al X-ray source at pressures of $\sim 5\times10^{-9}$ Torr. GNRs were then transferred to a SiO$_2$/Si substrate assisted by a spin-coated PMMA film and, after washing the PMMA with acetone, they were subjected to the functionalization processes. Functionalization with 4-NBD (Tokyo Chemical Industry, Japan) was carried out by immersing the samples for fixed times into 20 mM aqueous solutions. Immediately after the functionalization with diazonium has been completed, samples were rinsed in isopropanol and ultra-pure water to quench the reaction and remove any adsorbed molecules that may remain unreacted. For the functionalization with DETA (Sigma-Aldrich, USA) we followed a method reported elsewhere,[35] which consist in heating the sample at 70 °C for 30 minutes in an enclosed environment saturated with DETA vapor. For the sake of comparison, we conducted the same functionalization procedures with 4-NBD and DETA on uniform single-layer graphene sheets directly transferred on SiO$_2$/Si substrates after the CVD.

The evolution of the doping was followed by confocal Raman microscopy at a laser excitation wavelength of 532 nm (Nanofinder 30, Tokyo Instruments Inc.). Raman data was obtained from 20×20 μm^2 mappings composed of 1600 single spectra. The same area was mapping before and after each of the functionalization procedures, to allow for direct comparison. XPS was also used to confirm the functionalization to the aligned GNRs. To study the electronic
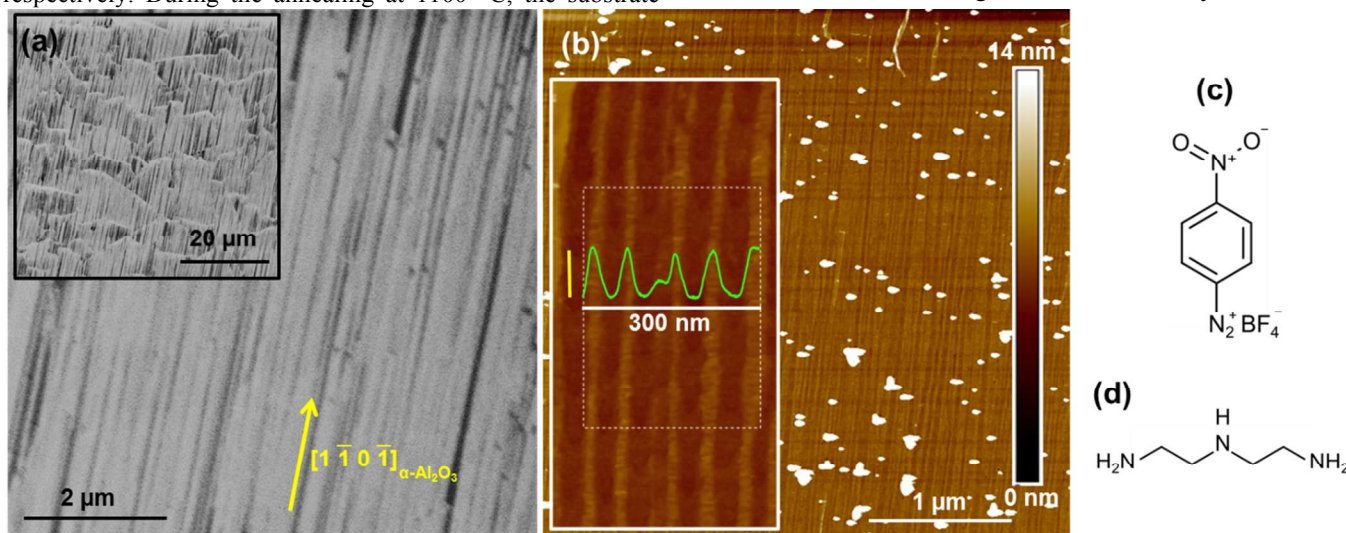
Fig. 1 (a) SEM image of the GNRs employed in this work (dark stripes) with a yellow arrow indicating the crystal direction of the sapphire substrate along which the etching proceeds. Inset shows a large-area SEM image of the GNRs. Light areas of the image correspond to the sapphire substrate. (b) AFM image of the GNRs. Inset in (b) shows a high resolution AFM image of the GNRs, with a 300 nm long height profile averaged within the white dotted box. Vertical yellow scale near the profile represents a height of 1 nm. Schematics of the molecules used for the functionalization of the GNRs: (c) 4-NBD and (d) DETA.
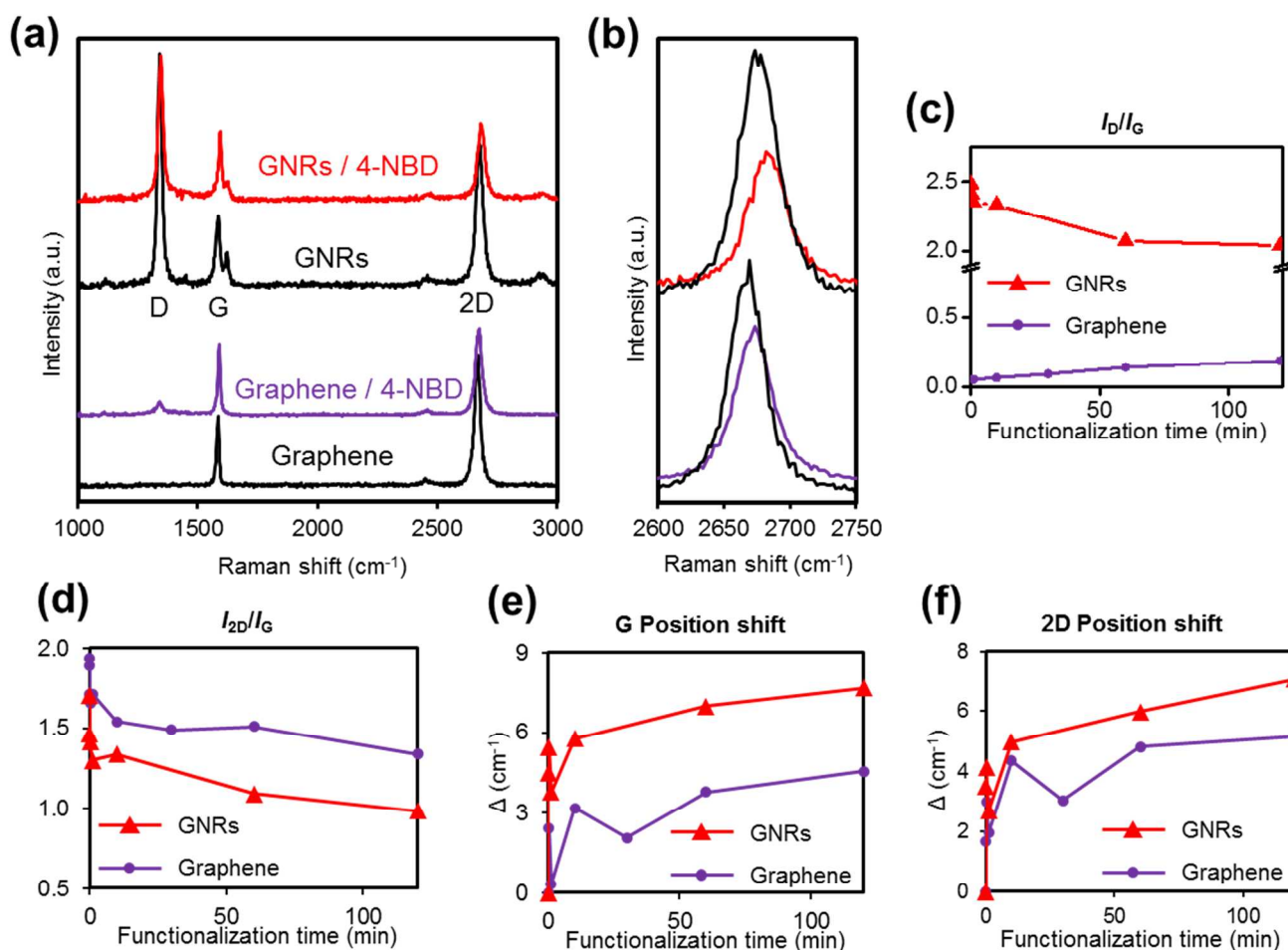
Fig. 2 (a, b) Raman spectra of (from bottom to top) graphene and GNRs both before (black) and after (purple, red) functionalization with 4-NBD for 2h. Spectra are normalized to the G band intensity and are vertically shifted for clarity. (a) General spectra, (b) 2D band region. Variation with functionalization time of (c) I_D/I_G, (d) I_{2D}/I_G, and shift of the (e) G and (f) 2D bands for graphene (purple circles) and GNRs (red triangles).

properties of the GNRs, 10 μm wide multichannel FET devices were fabricated, with channel lengths between 1 and 2 μm. For this purpose, electrode patterns were made by electron beam lithography, and Au was deposited by thermal evaporation. Carrier transport properties were measured at room temperature and under vacuum (~ 5×10^{-4} Pa) with a semiconductor parameter analyzer (Agilent B1500A).

Results and Discussion

p-Type doping of the GNRs by functionalization with 4-NBD

Figure 1a shows SEM images of the as-produced GNRs (dark parallel stripes in the image), made by Ni-assisted anisotropic etching of CVD-grown graphene supported on a sapphire r-plane substrate (light areas).[15] Ni nanoparticles react with the carbon atoms of graphene at elevated temperatures in a H_2 atmosphere (15% H_2 in Ar gas), producing etched lines in the graphene. When using sapphire r-plane as substrate, etching

proceeds along the [1 $\overline{1}$ 0 $\overline{1}$] direction of the sapphire,[15,41] thus leaving GNR arrays which are also oriented in the same direction. AFM inspection also reveals the production of high-density GNR arrays (Fig. 1b), with measured heights of ~1 nm. Figure 2a (upper, black spectrum) shows the Raman spectrum of the pristine GNRs on SiO_2/Si. The intensity of the Raman 2D band is approximately double than that of the G band ($I_{2D}/I_G \sim$ 2), and its full width at half maximum (FWHM) is narrow (~35 cm^{-1}). These results confirm that the nanoribbons are composed of single-layer graphene. Raman spectra also show a sharp and intense D band for the pristine GNRs, with most of it (approximately 80% of the intensity) originated from the presence of a large quantity of aligned edges within the Raman laser spot, as determined by previous polarization-dependent Raman studies.[15] The rest of the D-band signal is most likely ascribed to several factors, such as the roughness of the edges,[42] and to a partial hydrogenation or to structural damage of the graphene lattice produced during the etching process in H_2 at high temperature.[43,44]
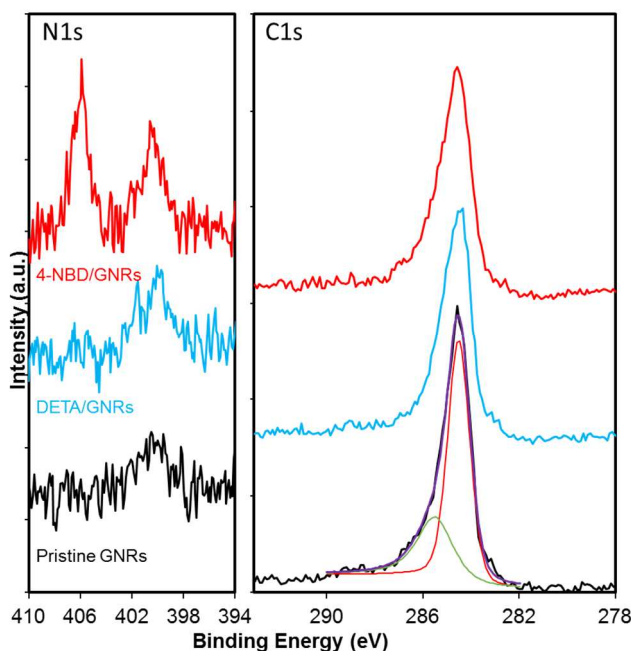
Fig. 3 XPS N1s (left) and C1s (right) spectra of (bottom to top) pristine, DETA, and 4-NBD functionalized GNRs. Bottom C1s spectrum shows the two components used for the fitting (in red and green), and their sum (purple).

In order to realize p-type doping of the GNRs we functionalized them with 4-NBD, which has been proved to be efficient for hole-doping of single-layer graphene sheets (see Fig. 1c for chemical structure of 4-NBD).[28,29,31] Functionalization of graphene with diazonium salts has been acknowledged to proceed mainly by the covalent attachment of the aryl radicals at basal plane and edge sites, with preference for the latter.[9,24,32,36,39] A charge transfer between the aryl group and the graphene is then produced, inducing a change in the doping level of the graphene that should depend on the nature of the functional group of the diazonium.[25,28,31,38] Because the 4-NBD molecule has an electron withdrawing nitro group (see Fig. 1c), hole doping is expected to occur in the GNRs.[5,28,31] Figure 3 presents the N1s and C1s regions of the XPS spectra of the GNRs measured before and after functionalization with 4-NBD for two hours. Functionalization did not produce big changes in the C1s band of the spectra, which were fitted with a main component at 284.5 eV, assigned to sp^2 carbon (for the fitting of the C1s bands refer to the Figure S1 of the Electronic Supplementary Information (ESI)). A second component was used, located at 285.5 eV. The origin of this component can have several sources, such as sp^3 hybridized bonds, C-N bonds, and contamination due to ambient exposure.[24,30] The success of the functionalization was determined by the increase of the nitrogen content by XPS, revealing the presence of the nitro groups from the 4-NBD. Two differentiated peaks appear in the N1s region after functionalization, located at ~ 404 eV and ~ 400 eV. The peak located at ~ 404 eV is ascribed to nitro groups of the attached aryl groups. The increase of intensity of the peak at 400 eV is probably due to the transformation of some of the nitro groups by the irradiation during the XPS collection.[24,33] The N:C atomic ratio of the GNRs clearly increased from 1:182 to 1:23 after functionalization with 4-NBD. The observed increase in the N:C ratio indicates the introduction of approximately 0.05 aryl groups per C atom of the GNRs.

Raman spectroscopy also evidenced the effects of the functionalization in the GNRs (compare the two upper spectra of Fig. 2a). We observed that the functionalization with 4-NBD results in a decrease of the relative intensity of the 2D band (Figs. 2b and 2d) and an upshift of both the G and 2D bands (Figs. 2e and 2f). The I_{2D}/I_G ratio is very sensitive to the carrier doping and is known to decrease with increasing doping levels.[35,45] In addition, the fact that both the G and 2D bands are shifted to higher wavenumbers implies a hole (p-type) doping of the GNRs.[42,45] The same behaviors were also observed for the functionalization of the pristine graphene, but the effects are stronger in our GNRs (see comparisons in Fig. 2d to 2f), indicating a higher doping for the latter. The fact that the doping effect is higher for the GNRs, points to the importance of the edges in the process of functionalization.[19,28,36]

For both graphene and GNRs, the I_{2D}/I_G ratio showed a noticeable change within the first minute of the treatment, after which it continues decreasing although at slower paces. The peak positions of G and 2D bands showed a similar tendency. Although the reason for this behavior is not completely clear, it may be related with the removal of residual PMMA generated during the transfer process of the graphene/GNRs to the SiO_2 substrate. It is commonly acknowledged that complete removal of PMMA residuals is a problematic issue, even after long periods of exposure to acetone.[46] Regarding this, as shown in Fig. S2 of the ESI, optical microscopy inspections revealed that short exposures to aryl diazonium can have a positive effect; removing polymer residuals present on the surface of the samples. Although inspection by optical microscopy and Raman measurements revealed that the quantity of polymer residuals in the relevant areas of the samples must be marginal, we cannot completely exclude its presence. We speculate that such unexpected removal of PMMA residue can lead to some of the observed changes in Raman within the first instants of the functionalization (see Fig. 2d to 2f).
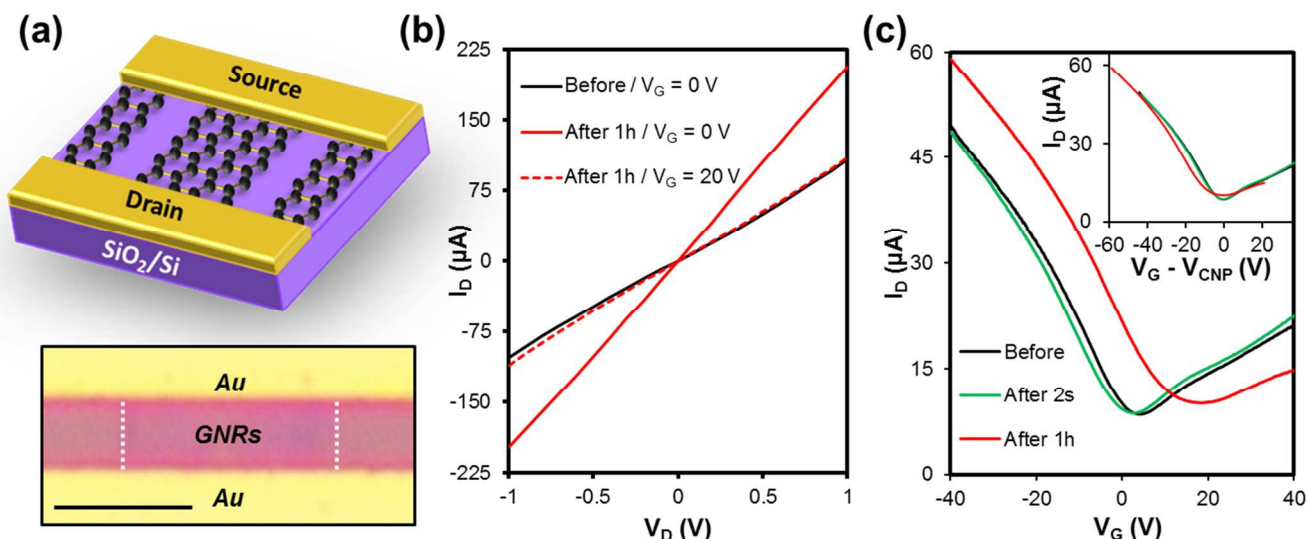
Fig. 4 (a) Schematic of a FET device (top), and an optical image of an actual device (bottom), with gold electrodes (yellow), and the GNR multi-channel between the dotted white lines (scale bar represents 5 μm). (b) Output characteristics of the GNRs with no gate voltage before and after functionalization (red and black lines respectively) and at a gate voltage of 20 V after functionalization (dotted red line). (c) Transfer characteristics of GNRs before (black) and after functionalization with 4-NBD for 2s (green) and 1h (red). Upper inset in (c) shows the same curves horizontally shifted to coincide the CNP.

Interestingly, it was observed that the relative intensity of the D band respect to the G band (I_D/I_G) for our GNRs decreases after the reaction with 4-NBD (upper red spectrum in Fig. 2a). This tendency is opposite from what would be expected given the covalent nature of the attachment, which normally increases the I_D/I_G ratio.[28,36,39] For comparison, we studied the 4-NBD functionalization of graphene under the same conditions and found that it induces the appearance of a D band, which was initially absent in the pristine spectrum (see Fig. 2a). As shown in Fig. 2c, one can see that the functionalization time dependences of the I_D/I_G ratio of GNRs and graphene show opposite trends. At the same time, functionalization with 4-NBD did not induce the appearance of any diazonium-related band in the Raman spectra of our GNRs. These bands, mainly located at ~ 1400 and ~ 1440 cm^{-1}, originated from surface-adsorbed non-covalently reacted diazonium molecules.[26,28] The lack of diazonium-related bands in our spectra confirms the formation of covalent bonds between the GNRs and 4-NBD. The explanation for the apparent contradiction between the behavior of the I_D/I_G ratio and the lack of extra Raman bands, is that grafting of the aryl groups is predominantly at the edges of the GNRs. Edges are supposed to have a higher reactivity than the basal plane,[19,28,36] and in our case they are playing a fundamental role in the functionalization, as evidenced by the lower doping attained in graphene (compare trends in Fig. 2d to 2f). Another possibility is the exchange with preexisting attached functional groups or atoms (mainly hydrogen) at both basal and edge sites. In both cases I_D/I_G does not necessarily increase, as no new sp^3 bonds need to be produced. In agreement, the relative intensity of the component associated with sp^2 bonding in the XPS signal of the C1s peak does not change after functionalization, indicating that the amount of sp^2 bonds remains unaltered.[30] The fact that aryl groups are bonding mainly to the edges, allows us to control the doping level of the ribbons by covalent functionalization. The binding of the aryl groups to the edges of the GNRs does not adequately explain the observed net decrease of the I_D/I_G ratio. As discussed below, we attribute this decrease of the relative intensity of the D band to the effects of the doping in the Raman spectra.

The evolution of the electronic properties of the GNRs was evaluated by measuring the performance of multichannel GNR-FET devices (see schematic in Fig. 4a) before and after functionalization with 4-NBD. Solid curves in Figure 4b show the output characteristics of the GNRs with no gate voltage applied, showing that functionalization results in an increase of the conductivity. The transfer curves in Fig. 4c indicate that the charge neutrality point (CNP) shifts ~ 23.3 ± 10.9 V towards higher gate voltage values after one hour of functionalization. The output curve of the functionalized GNRs at a gate voltage of 20 V almost completely matches that before functionalization with no gate voltage (Fig. 4b). This indicates that the functionalization with 4-NBD effectively induces hole doping of the GNRs, in consistent with the Raman results. Functionalization of covalent nature is in principle expected to result in a decrease of the conductivity of the GNRs, which would be observed as a decrease of the drain current at the CNP.[9,26,39] However, we observed that the current slightly increases after the functionalization (inset of Fig. 4c, average increase of 15% measured in different devices). Although the origin of this increase is not clear, some reports indicate that it may be linked to the increase of the carrier density after attachment of the aryl groups.[29,47] It is worth pointing out here that as aryl groups are bonding mainly to the edges and the quantity of new defects created is small, we can attain covalent functionalization without degrading the original electronic properties of the GNRs.

It is noteworthy that several studies suggest that the nature of the radical in the diazonium salt can determine the kind of doping produced.[25,28,31,38] Thus, replacing the nitro group present in the 4-NBD by a methoxy group should change the doping to n-type.[25,31] However, functionalization of our GNRs with 4-methoxybenzenediazonium (4-MBD) did not produce the expected n-type doping, and our results indicate that hole doping is being produced instead (refer to the ESI and Figs. S3 and S4 for a more detailed discussion and data).[29]

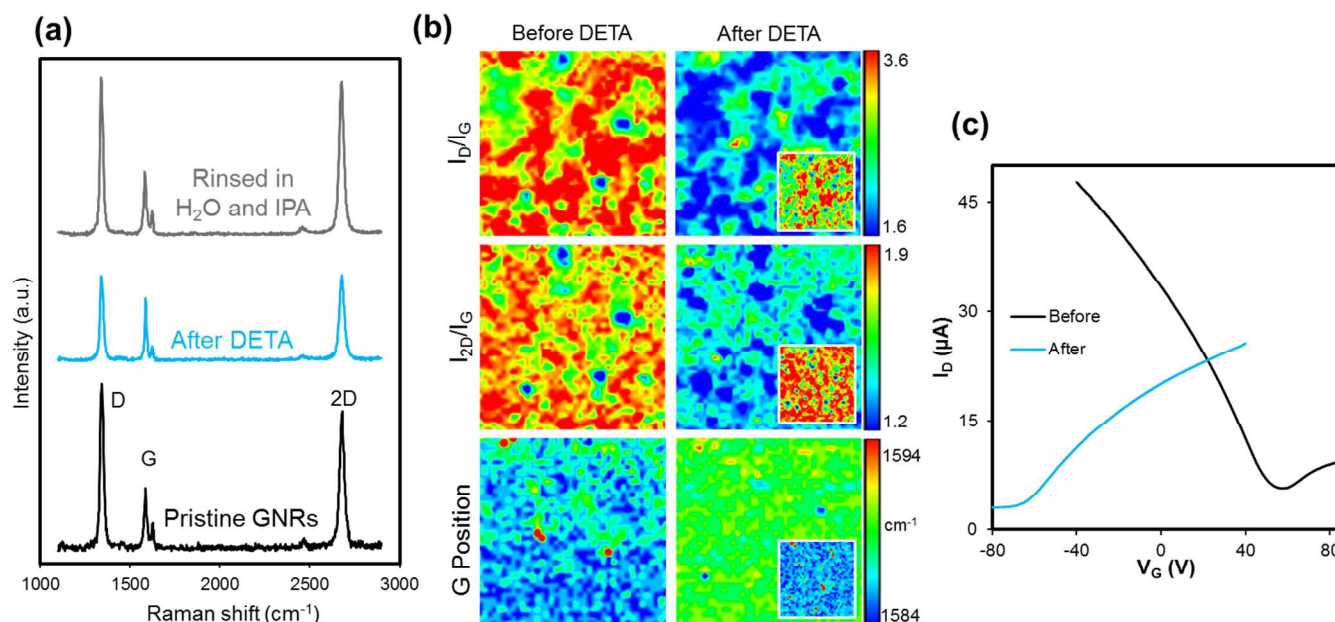## n-Type doping of the GNRs by functionalization with DETA

In order to induce n-type doping in the aligned GNRs, we found exposure to DETA (molecule represented in Fig. 1d) in vapor form to be very effective, as presented in Fig. 5. The functionalization is expected to proceed by the adsorption of the DETA molecules on the GNRs without forming covalent bonds, as has been reported to occur for graphene sheets.[21,35] After functionalization of the GNRs with DETA, the N:C atomic ratio measured by XPS increased to 1:67 from an initial value of 1:182 (see Fig. 3). An increase of intensity of the N1s band occurs at binding energies around ~ 400 eV, which is compatible with the presence of amine groups from the DETA molecule.[24] This increase indicates a concentration of approximately 0.03 DETA molecules per C atom of the GNRs.

Raman spectra also showed evidence of the doping, with an upshift of the G band of ~ 2.9 cm^{-1}, and a decrease of the I_{2D}/I_G ratio from ~ 2.2 to ~ 1.3 (Fig. 5a). Raman mapping over an area of 400 μm^2 show that functionalization proceeds uniformly across the surface (Fig. 5b). The position of the 2D band also upshifted, although in contrast to the case of 4-NBD, the shift is considerably smaller than that of the G band (~ 0.4 cm^{-1}). The observed changes in Raman spectra are larger than those produced on pristine graphene under the same conditions (see Fig. S5 of the ESI), which again indicates a higher reactivity of the GNRs as in the case of functionalization with 4-NBD. Surprisingly, the I_D/I_G ratio decreased to almost the half after functionalization with DETA, a bigger change than occurring in the case of 4-NBD. As will be shown, FET measurements demonstrate a strong n-type doping of the GNRs after functionalization, which is compatible with the Raman observations. It should be noted that the Raman measurements

were performed in air whereas the transport measurements were done in vacuum (~ 5×10^{-4} Pa), and thus it is expected a decreased n-type character in the former due to unintentional p-doping under ambient conditions.[48] It is also worth noting that as the pristine GNRs have a weak p-type character, the net variations in the Raman parameters associated to the degree of doping (such as the I_{2D}/I_G ratio and the position of the bands) are expected to be smaller than those expected if the GNRs were initially in a non-doped state.[34]

The study of the transfer characteristics of the GNRs functionalized with DETA clearly demonstrated the strong n-type character attained (Fig. 5c). Although the initial position of the CNP varies across different devices, it always located at positive values of the gate voltage, indicating that initially the GNRs are unintentionally p-type doped. This phenomenon is commonly reported in the case of graphene and has been ascribed to the presence of adsorbed ambient water and other impurities.[34,48] After functionalization with DETA, the CNP of the FET shifts to negative values of the gate voltage, implying an n-type doping. The observed shifts were of ~ 136.9 ± 0.4 V, with the CNP lying at around -75 V after the functionalization. The electron donating amine groups present in the DETA molecule are expected to cause such high n-type doping. It should be noted that the degree of doping can be probably tuned finely by choosing a different ethylene amine, or by changing the conditions of the exposure, such as the time or the temperature.

Graphene doped with ethylene amines has been reported to gradually lose its doping character when exposed to air for long periods, as those molecules easily react with water vapor present in air.[35] In our case, the doped state of our GNRs showed high stability after 2 weeks stored in vacuum (~ 5×10^{-4} Pa) at ambient temperature, with no evident signs of a decrease in the strength of the doping character. To test the effects of water, some samples were rinsed in ultrapure water and

Fig. 5 (a) Representative Raman spectra of the GNRs before (black), after functionalization with DETA (blue), and after rinsing in H$_2$O and isopropanol (gray). (b) Raman mappings of the same area (20 × 20 μm^2) before (left column) and after functionalization (right column), and after rinsing in H$_2$O and isopropanol (insets). (c) Transfer characteristics of a GNR-FET before (black) and after functionalization with DETA (orange).

isopropanol after being functionalized with DETA. Raman characterization showed that the samples recover almost completely their previous characteristics, as can be seen in Fig. 5a. Most notably, the ratios I_D/I_G and I_{2D}/I_G decrease to below 60% of their original values after DETA functionalization, and recover to approximately 94% after washing. Raman mappings of the same area collected during each of the stages show that the recovery after washing is mostly uniform (Fig. 5b, and Fig. S6a of the ESI). FET measurements also showed a shift of the CNP towards zero gate voltages.

Behavior of the I_D/I_G ratio for the functionalized GNRs

As already mentioned, an unexpected decrease of I_D/I_G was observed in the Raman spectra of the GNRs after functionalization with 4-NBD and DETA (see Figs. 2a and 5a). It is known that in the presence of point defects in graphene, the I_D/I_G ratio increases with the concentration of defects until it reaches a maximum value.[49–51] Once this maximum is reached, the trend is reverted and further increases of the defect density induce a lowering of the I_D/I_G ratio. This does not seems to be the case of our GNRs for several reasons. First, this is valid for point defects, but in our case most of the D band seems to be originated in the edges of the GNRs. Thus, the possible contribution of point defects to the D band is not high enough to be so close to that maximum. Second, in the presence of such high density of defects, the decrease of I_D/I_G is usually accompanied by a degradation of the second order 2D peak,[51] but this was not observed for our GNRs. Third, in this regime it would be reasonable to expect a significant decrease in conductivity,[52] which was not observed in FET measurements. Lastly, we observed this phenomenon for both 4-NBD and DETA functionalization, which present different mechanisms of functionalization.

Taking into account these arguments, it seems that the change in the I_D/I_G ratio for the functionalized GNRs cannot be completely ascribed to a variation in the quantity of covalent attached functional groups. The reason for the decrease of I_D/I_G is not clear, but possibly is an effect caused by the doping of the GNRs. Doping of graphene has been reported to change the intensity of the G band,[42] which indeed is one of the causes of the decrease of the I_{2D}/I_G ratio. But under certain circumstances, such as high doping, may also have some noticeable effect in the I_D/I_G ratio. In fact, a decrease in the relative intensity of the D band has been reported in highly doped carbon nanotubes,[53] and more recently in gate-induced doping experiments in defective graphene.[54,55] In these studies no new defects are introduced in the graphitic lattice during the doping, and the decrease of the I_D/I_G is exclusively due to the doping. Therefore, in the general case of covalent functionalization of graphitic materials, the net variation of the I_D/I_G ratio is expected to arise from a competition between the effect of the introduction of sp^3 bonds (tending to increase the ratio) and the doping effect of the attached groups (decreasing that ratio).

Although the difference in the doping levels attained for each case prevent a quantitative comparison, our observations agree well with this assumption. Thus, our results seem to corroborate that net changes in I_D/I_G come from the relative importance of doping and variation of defects in each case. Consequently, we observe the highest decrease of the I_D/I_G ratio in the case of the functionalization of GNRs with DETA (see Fig. 5a), for which the doping is expected to dominate as no defects are created. A decrease is even observed in the case of graphene functionalized with DETA, for which the D band is

usually negligible (see Fig. S5). In the functionalization of the GNRs with 4-NBD, the I_D/I_G still decreases, but in a smaller quantity than for DETA (Fig. 2a). This is an indication that the small quantity of new defects that may be introduced are not enough to compensate for the effects of doping, as expected in case that aryl groups mainly attach to the edges of the GNRs. On the other hand, we observed a slight increase of the I_D/I_G ratio during the functionalization of the GNRs with 4-MBD, for which the doping effects are smaller than for the case of 4-NBD (see Fig S4c of the ESI). Thus, it seems that the contribution of the newly created sp^3 bonds in this case is enough to compensate for the doping effect, thus producing a net increase of the I_D/I_G ratio. Lastly, functionalization of a graphene sheet with 4-NBD induced the biggest increase in the I_D/I_G ratio (Fig. 2a). This is explained by the fact that for graphene, every attached aryl group needs to create a defect, something that does not occur for the GNRs. Thus, in this case the contribution of the defects highly outweighs that of the doping, producing the observed increase.

All the mentioned above indicates that Raman spectra must be carefully interpreted when doping and defects are present in graphitic materials, and should be accompanied by complementary studies.

Conclusions

We demonstrate that controlled doping of GNRs can be attained by chemical functionalization. By selecting the functional agent, tuning of the doping level from n- to p-type can be easily produced. Doping effects on the GNRs were higher than those of graphene functionalized under the same conditions. This indicates the importance of the edges in the functionalization of the GNRs, increasing the reactivity and facilitating the functionalization. In this sense, as the functional groups react preferentially with the edges of the GNRs, even covalent functionalization can be produced without further degrading the electronic performance of the GNRs. It was also shown that Raman data should be carefully interpreted in the general case of functionalizing sp^2 based materials, as the introduction of functional groups and their doping effect compete to modulate the ratio of the D and G bands. Our results of controlled doping of GNRs are expected to facilitate the production of nanoribbon-based p-n junctions by controlled localized functionalization.

Notes and references

[a] Institute for Materials Chemistry and Engineering (IMCE), Kyushu University, Kasuga, Fukuoka 816-8580, Japan.

[b] PRESTO, Japan Science and Technology Agency (JST), Kawaguchi, Saitama 243-0198, Japan.

[†] Current address: Faculty of Engineering and Physical Sciences, School of Chemistry, University of Manchester, Manchester M13 9PL, UK.

* Corresponding author: Prof. Hiroki Ago, e-mail address: ago@cm.kyushu-u.ac.jp

1   Y. Zhang, T.-T. Tang, C. Girit, Z. Hao, M. C. Martin, A. Zettl, M. F. Crommie, Y. R. Shen and F. Wang, *Nature*, 2009, **459**, 820.
2   Z. H. Ni, T. Yu, Y. H. Lu, Y. Y. Wang, Y. P. Feng and Z. X. Shen, *ACS Nano*, 2008, **2**, 2301.
3   J. Park, S. B. Jo, Y.-J. Yu, Y. Kim, J. W. Yang, W. H. Lee, H. H. Kim, B. H. Hong, P. Kim, K. Cho and K. S. Kim, *Adv. Mater.*, 2012, **24**, 407.
4   R. Balog, B. Jørgensen, L. Nilsson, M. Andersen, E. Rienks, M. Bianchi, M. Fanetti, E. Lægsgaard, A. Baraldi, S. Lizzit, Z. Sljivancanin, F. Besenbacher, B. Hammer, T. G. Pedersen, P. Hofmann and L. Hornekær, *Nat. Mater.*, 2010, **9**, 315.
5   S. Niyogi, E. Bekyarova, M. E. Itkis, H. Zhang, K. Shepperd, J. Hicks, M. Sprinkle, C. Berger, C. N. Lau, W. A. deHeer, E. H. Conrad and R. C. Haddon, *Nano Lett.*, 2010, **10**, 4061.
6   X. Li, X. Wang, L. Zhang, S. Lee and H. Dai, *Science*, 2008, **319**, 1229.
7   N. Camara, J.-R. Huntzinger, G. Rius, A. Tiberj, N. Mestres, F. Pérez-Murano, P. Godignon and J. Camassel, *Phys. Rev. B*, 2009, **80**, 125410.
8   J. Cai, P. Ruffieux, R. Jaafar, M. Bieri, T. Braun, S. Blankenburg, M. Muoth, A. P. Seitsonen, M. Saleh, X. Feng, K. Müllen and R. Fasel, *Nature*, 2010, **466**, 470.
9   A. Sinitskii, A. Dimiev, D. A. Corley, A. A. Fursina, D. V. Kosynkin and J. M. Tour, *ACS Nano*, 2010, **4**, 1949.
10 L. Jiao, L. Xie and H. Dai, *Nano Res.*, 2012, **5**, 292.
11 H. Ago, Y. Ito, M. Tsuji and K. Ikeda, *Nanoscale*, 2012, **4**, 5178.
12 T. Kato and R. Hatakeyama, *Nat. Nanotechnol.*, 2012, **7**, 651.
13 X. Liang and S. Wi, *ACS Nano*, 2012, **6**, 9700.
14 H. Ago, I. Tanaka, Y. Ogawa, R. M. Yunus, M. Tsuji and H. Hibino, *ACS Nano*, 2013, **7**, 10825.
15 P. Solís-Fernández, K. Yoshida, Y. Ogawa, M. Tsuji and H. Ago, *Adv. Mater.*, 2013, **25**, 6562.
16 J. G. Son, M. Son, K.-J. Moon, B. H. Lee, J.-M. Myoung, M. S. Strano, M.-H. Ham and C. A. Ross, *Adv. Mater.*, 2013, **25**, 4723.
17 A. N. Abbas, G. Liu, B. Liu, L. Zhang, H. Liu, D. Ohlberg, W. Wu and C. Zhou, *ACS Nano*, 2014, **8**, 1538.
18 H. Ago, Y. Kayo, P. Solís-Fernández, K. Yoshida and M. Tsuji, *Carbon*, 2014, **78**, 339.
19 X. Wang, X. Li, L. Zhang, Y. Yoon, P. K. Weber, H. Wang, J. Guo and H. Dai, *Science*, 2009, **324**, 768.
20 F. Bonaccorso, Z. Sun, T. Hasan and A. C. Ferrari, *Nat. Photonics*, 2010, **4**, 611.
21 T. O. Wehling, K. S. Novoselov, S. V. Morozov, E. E. Vdovin, M. I. Katsnelson, A. K. Geim and A. I. Lichtenstein, *Nano Lett.*, 2008, **8**, 173.
22 F. Traversi, V. Russo and R. Sordan, *Appl. Phys. Lett.*, 2009, **94**, 223312.
23 M. L. Usrey, E. S. Lippmann and M. S. Strano, *J. Am. Chem. Soc.*, 2005, **127**, 16129.
24 E. Bekyarova, M. E. Itkis, P. Ramesh, C. Berger, M. Sprinkle, W. A. de Heer and R. C. Haddon, *J. Am. Chem. Soc.*, 2009, **131**, 1336.
25 F. M. Koehler, N. A. Luechinger, D. Ziegler, E. K. Athanassiou, R. N. Grass, A. Rossi, C. Hierold, A. Stemmer and W. J. Stark, *Angew. Chem. Int. Ed.*, 2009, **48**, 224.
26 D. B. Farmer, R. Golizadeh-Mojarad, V. Perebeinos, Y.-M. Lin, G. S. Tulevski, J. C. Tsang and P. Avouris, *Nano Lett.*, 2009, **9**, 388.
27 V. Georgakilas, M. Otyepka, A. B. Bourlinos, V. Chandra, N. Kim, K. C. Kemp, P. Hobza, R. Zboril and K. S. Kim, *Chem. Rev.*, 2012, **112**, 6156.
28 F. M. Koehler, A. Jacobsen, K. Ensslin, C. Stampfer and W. J. Stark, *Small*, 2010, **6**, 1125.
29 E. Pembroke, G. Ruan, A. Sinitskii, D. A. Corley, Z. Yan, Z. Sun and J. M. Tour, *Nano Res.*, 2013, **6**, 138.
30 Q. Wu, Y. Wu, Y. Hao, J. Geng, M. Charlton, S. Chen, Y. Ren, H. Ji, H. Li, D. W. Boukhvalov, R. D. Piner, C. W. Bielawski and R. S. Ruoff, *Chem. Commun.*, 2013, **49**, 677.
31 M. A. Bissett, S. Konabe, S. Okada, M. Tsuji and H. Ago, *ACS Nano*, 2013, **7**, 10335.
32 G. L. C. Paulus, Q. H. Wang and M. S. Strano, *Acc. Chem. Res.*, 2013, **46**, 160.
33 L. Zhang, J. Yu, M. Yang, Q. Xie, H. Peng and Z. Liu, *Nat. Commun.*, 2013, **4**, 1443.
34 P. Wei, N. Liu, H. R. Lee, E. Adijanto, L. Ci, B. D. Naab, J. Q. Zhong, J. Park, W. Chen, Y. Cui and Z. Bao, *Nano Lett.*, 2013, **13**, 1890.
35 Y. Kim, J. Ryu, M. Park, E. S. Kim, J. M. Yoo, J. Park, J. H. Kang and B. H. Hong, *ACS Nano*, 2014, **8**, 868.
36 R. Sharma, J. H. Baik, C. J. Perera and M. S. Strano, *Nano Lett.*, 2010, **10**, 398.
37 H. Zhang, E. Bekyarova, J.-W. Huang, Z. Zhao, W. Bao, F. Wang, R. C. Haddon and C. N. Lau, *Nano Lett.*, 2011, **11**, 4047.
38 Y.-J. Do, J.-H. Lee, H. Choi, J.-H. Han, C.-H. Chung, M.-G. Jeong, M. S. Strano and W.-J. Kim, *Chem. Mater.*, 2012, **24**, 4146.
39 C.-J. Shih, Q. H. Wang, Z. Jin, G. L. C. Paulus, D. Blankschtein, P. Jarillo-Herrero and M. S. Strano, *Nano Lett.*, 2013, **13**, 809.
40 B. Hu, H. Ago, Y. Ito, K. Kawahara, M. Tsuji, E. Magome, K. Sumitani, N. Mizuta, K. Ikeda and S. Mizuno, *Carbon*, 2012, **50**, 57.
41 T. Tsukamoto and T. Ogino, *J. Phys. Chem. C*, 2011, **115**, 8580.
42 A. C. Ferrari and D. M. Basko, *Nat. Nanotechnol.*, 2013, **8**, 235.
43 T. Zecho, A. Horn, J. Biener and J. Küppers, *Surf. Sci.*, 1998, **397**, 108.
44 D. C. Elias, R. R. Nair, T. M. G. Mohiuddin, S. V. Morozov, P. Blake, M. P. Halsall, A. C. Ferrari, D. W. Boukhvalov, M. I. Katsnelson, A. K. Geim and K. S. Novoselov, *Science*, 2009, **323**, 610.
45 A. Das, S. Pisana, B. Chakraborty, S. Piscanec, S. K. Saha, U. V. Waghmare, K. S. Novoselov, H. R. Krishnamurthy, A. K. Geim, A. C. Ferrari and A. K. Sood, *Nat. Nanotechnol.*, 2008, **3**, 210.
46 J. W. Suk, W. H. Lee, J. Lee, H. Chou, R. D. Piner, D. Hao, D. Akinwande and R. S. Ruoff, *Nano Lett.*, 2013, **13**, 1462.
47 P. Huang, H. Zhu, L. Jing, Y. Zhao and X. Gao, *ACS Nano*, 2011, **5**, 7945.
48 K. S. Novoselov, A. K. Geim, S. V. Morozov, D. Jiang, Y. Zhang, S. V. Dubonos, I. V. Grigorieva and A. A. Firsov, *Science*, 2004, **306**, 666.
49 A. C. Ferrari and J. Robertson, *Phys. Rev. B*, 2000, **61**, 14095.
50 M. M. Lucchese, F. Stavale, E. H. M. Ferreira, C. Vilani, M. V. O. Moutinho, R. B. Capaz, C. A. Achete and A. Jorio, *Carbon*, 2010, **48**, 1592.
51 I. Childres, L. A. Jauregui, J. Tian and Y. P. Chen, *New J. Phys.*, 2011, **13**, 025008.
52 R. Rozada, P. Solís-Fernández, J. I. Paredes, A. Martínez-Alonso, H. Ago and J. M. D. Tascón, *Carbon*, 2014, **79**, 664.
53 M. Kalbac and L. Kavan, *Carbon*, 2010, **48**, 832.
54 J. Liu, Q. Li, Y. Zou, Q. Qian, Y. Jin, G. Li, K. Jiang and S. Fan, *Nano Lett.*, 2013, **13**, 6170.
55 M. Bruna, A. K. Ott, M. Ijäs, D. Yoon, U. Sassi and A. C. Ferrari, *ACS Nano*, 2014, **8**, 7432.